Simulations

In this supplementary document, comparisons towards other segmentation algorithms are presented. We compare our simulation results on the BSDS500 test set in Sec A.1 with other algorithms. Moreover, we further run simulations on the real-world images that covers all kinds of scenarios in Sec A.2 to justify that under any circumstances, both our proposed algorithms can perform highly accurate and fast superpixel merging techniques to produce good generic image segmentation results.

A.1 BSDS500

Fig. A.1 and Fig. A.2 show the comparison between the proposed methods and other methods like a deep-learning-based method, the W-Net, and classical segmentation algorithm gPb-OWT-UCM. As we can see, both the results of the proposed algorithms are much better than that of state-of-the-art algorithms, since ours can produce more general and compact segmentation results compared to the others.

In Fig. A.3 and Fig. A.4, we show another visual comparison of the proposed algorithms to DC-Seg-full, which is a famous learning-based method. Compare to the results of DC-Seg-full, the proposed methods can produce more compact and reliable segmentation.

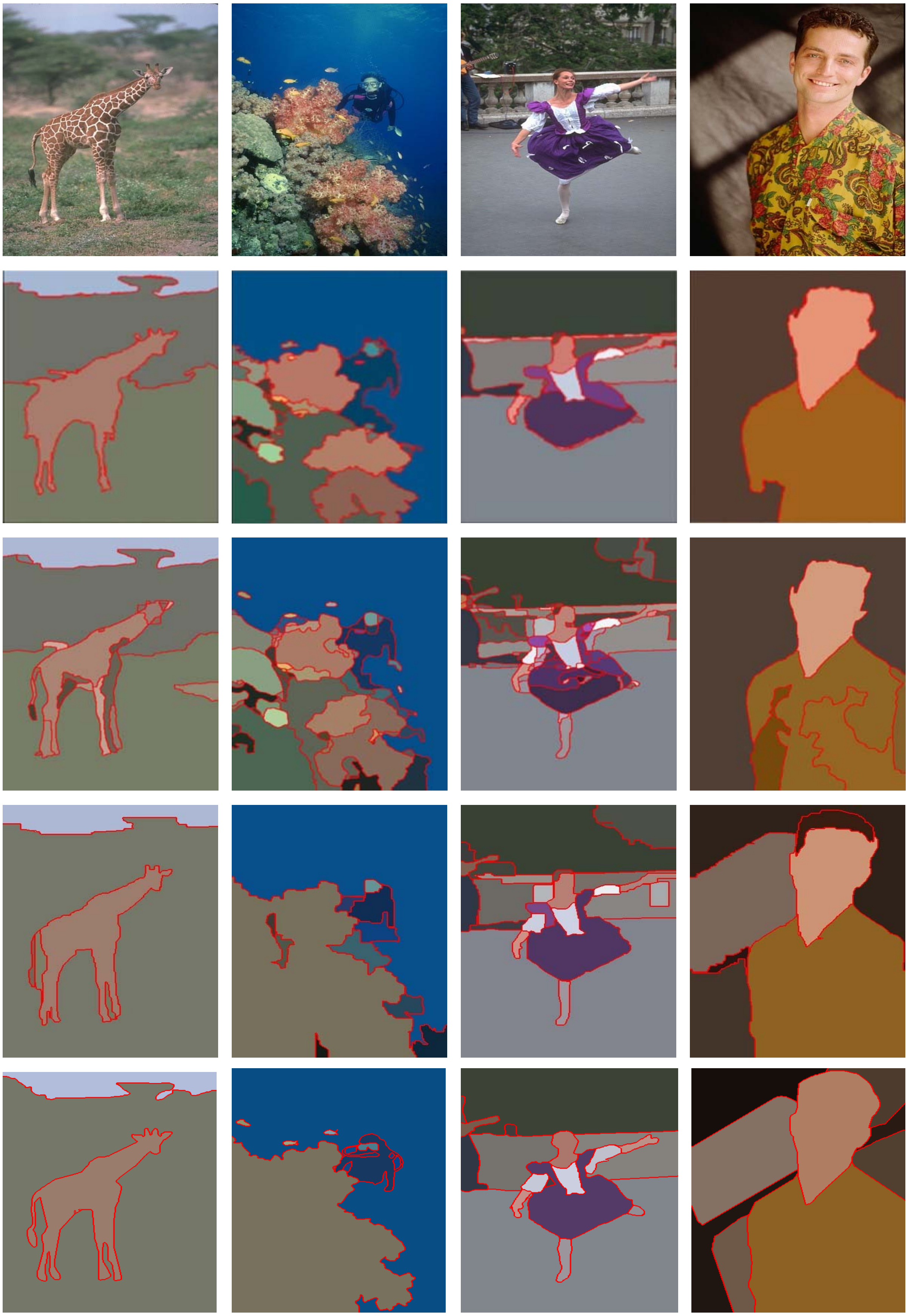

Figure A.1: Visual comparison between WNet, gPb-OWT-UCM, and the proposed *DMMSS-FCN*. (1^{st} row): original images. Results produced by (2^{nd} row): WNet; (3^{rd} row): gPb-OWT-UCM; (4^{th} row): *DMMSS-FCN(ours)*; (5^{th} row): *GroundTruth*.

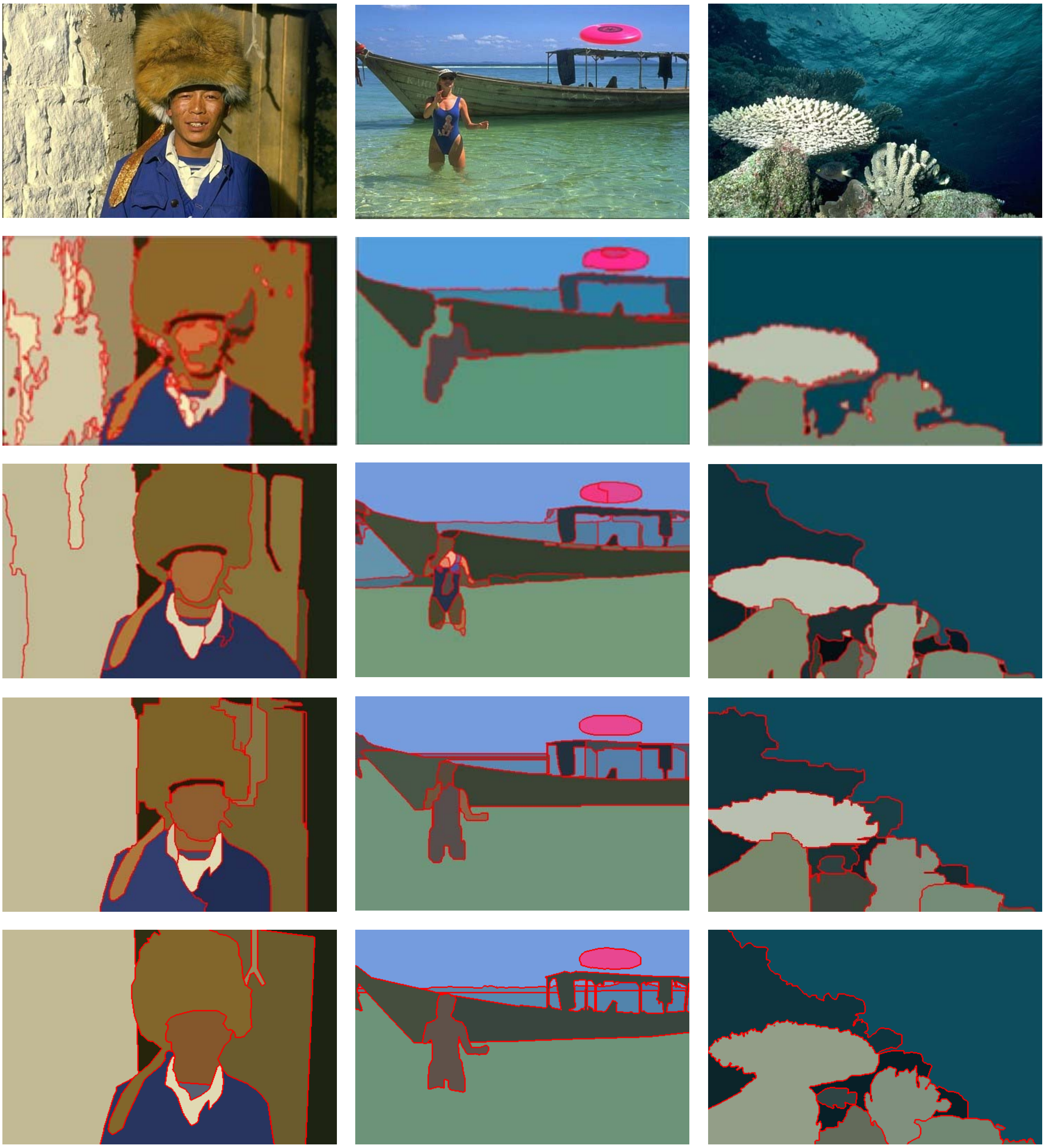

Figure A.2: Visual comparison between WNet, gPb-OWT-UCM, and the proposed *DMMSS-FCN*. (1^{st} row): original images. Results produced by (2^{nd} row): WNet; (3^{rd} row): gPb-OWT-UCM; (4^{th} row): *DMMSS-FCN(ours)*; (5^{th} row): *GroundTruth*.

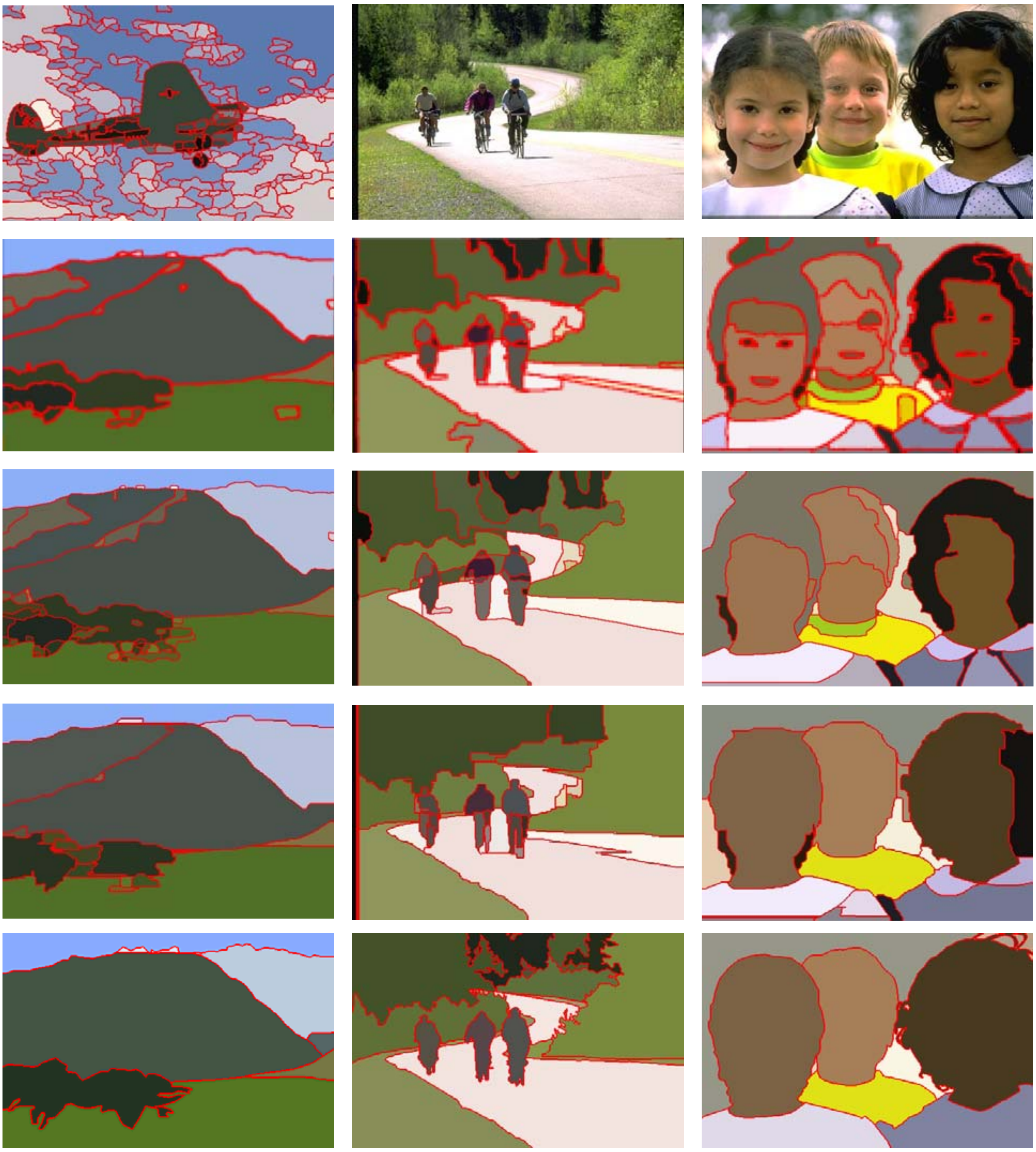

Figure A.3: Visual comparison between DC-Seg-full, and the proposed *DMMSS-FCN*. (1st row): original images. Results produced by (2nd row): DC-Seg-full; (3rd row): gPb-OWT-UCM; (4th row): *DMMSS-FCN(ours)*; (5th row): *GroundTruth*.

Figure A.4: Visual comparison between DC-Seg-full, and the proposed *DMMSS-FCN*. (1^{st} row): original images. Results produced by (2^{nd} row): DC-Seg-full; (3^{rd} row): gPb-OWT-UCM; (4^{th} row): *DMMSS-FCN(ours)*; (5^{th} row): *GroundTruth*

A.2 Real-World Images

In the following articles, we show that not only our models can outperform the state-of-the-art algorithms in BSDS500 dataset which we train our models from, but also in real-world scenarios. Therefore, we collected several types of images to prove that our proposed methods can maintain great performance over unseen data. In BSDS500, there are many classes of nature images within this dataset, making it a great benchmark and training source for learning image segmentation tasks. Nevertheless, there are too many classes among this world, it is difficult for a dataset to cover them all. Therefore, it is important for every deep-learning model to be bias-invariant. To verify that, we test both our proposed algorithms on modern real-world images.

A.2.1 Animals

Since our training set contains many nature images, our proposed methods are able to produce outstanding segmentation results. See Fig. A.7 for segmentation results on animal images compared to gPb-OWT-UCM.

A.2.2 Night View

In this section, we show some segmentation results on the images taken in the night to test the capability of our proposed methods of handling dark view scenario. In Fig. A.8, one can see that, our models manages to merge blur and low-luminance parts into compact objects while the other method fails to recognize such information and cause severe segmentation leakage. Therefore, such examples prove that our models are robust not only in images taken under great exposures, but in those low-light and blurry scenarios.

A.2.3 Items and Objects

We specifically pick some items and objects that are few in number or never been in our training set for testing. In the left column of Fig. A.9, we present simulations of an aircraft engine, which is difficult for another algorithm to perform accurate segmentation on the boundary of engine itself since the background information is similar to the engine. Nevertheless, both our proposed methods can generate compact segmentation without losing edge information. Moreover, food category such like coffee and snacks are never been shown in the training images. However, reliable segmentation result can still be produced by our methods. Fig. A.10 shows more examples of items and objects, on the left-most column, our methods successfully segmented the saliency part of the image, which is the stone.

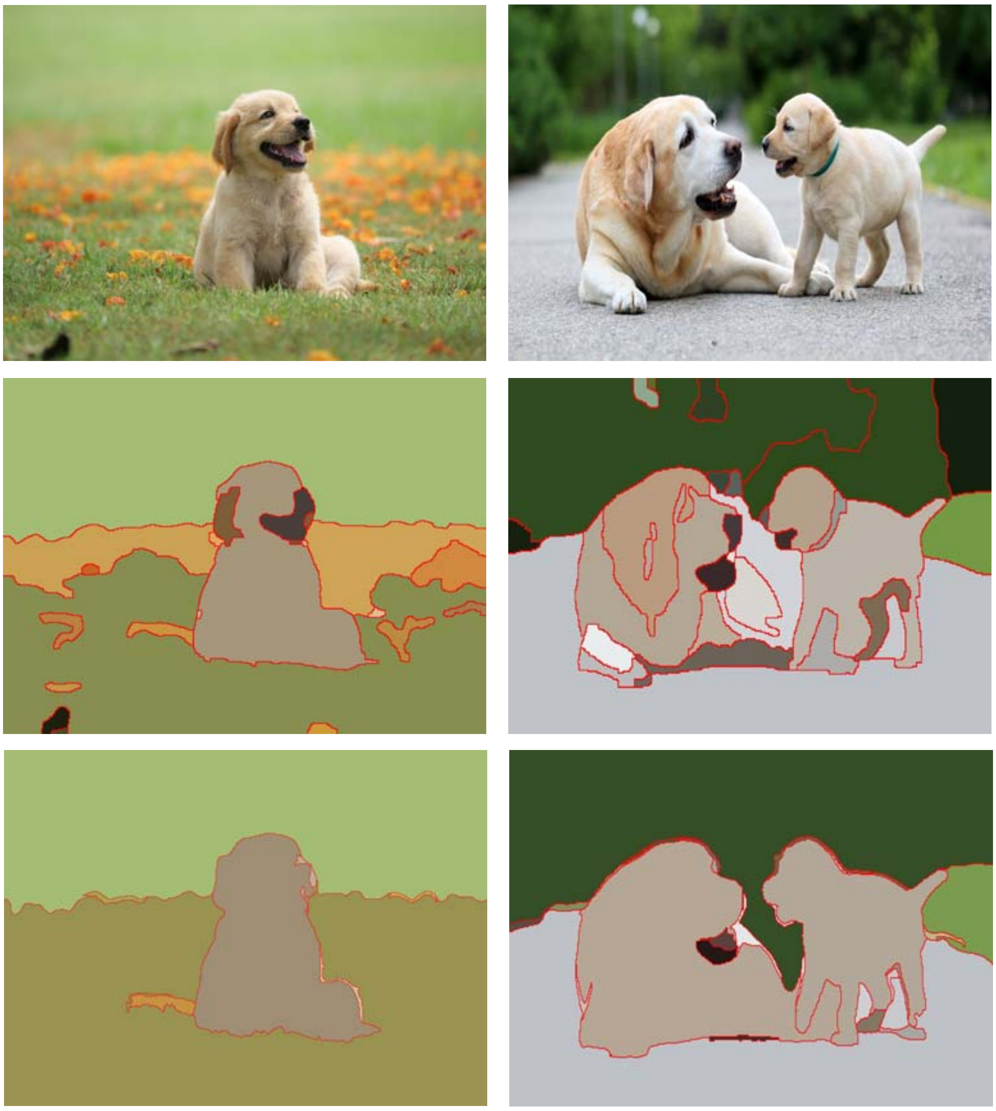

Figure A.7: Real-world animal image segmentation results. (1^{st} row): original images. Results produced by (2^{nd} row): gPb-OWT-UCM [4]; (4^{th} row): *DMMSS-FCN(ours)*.

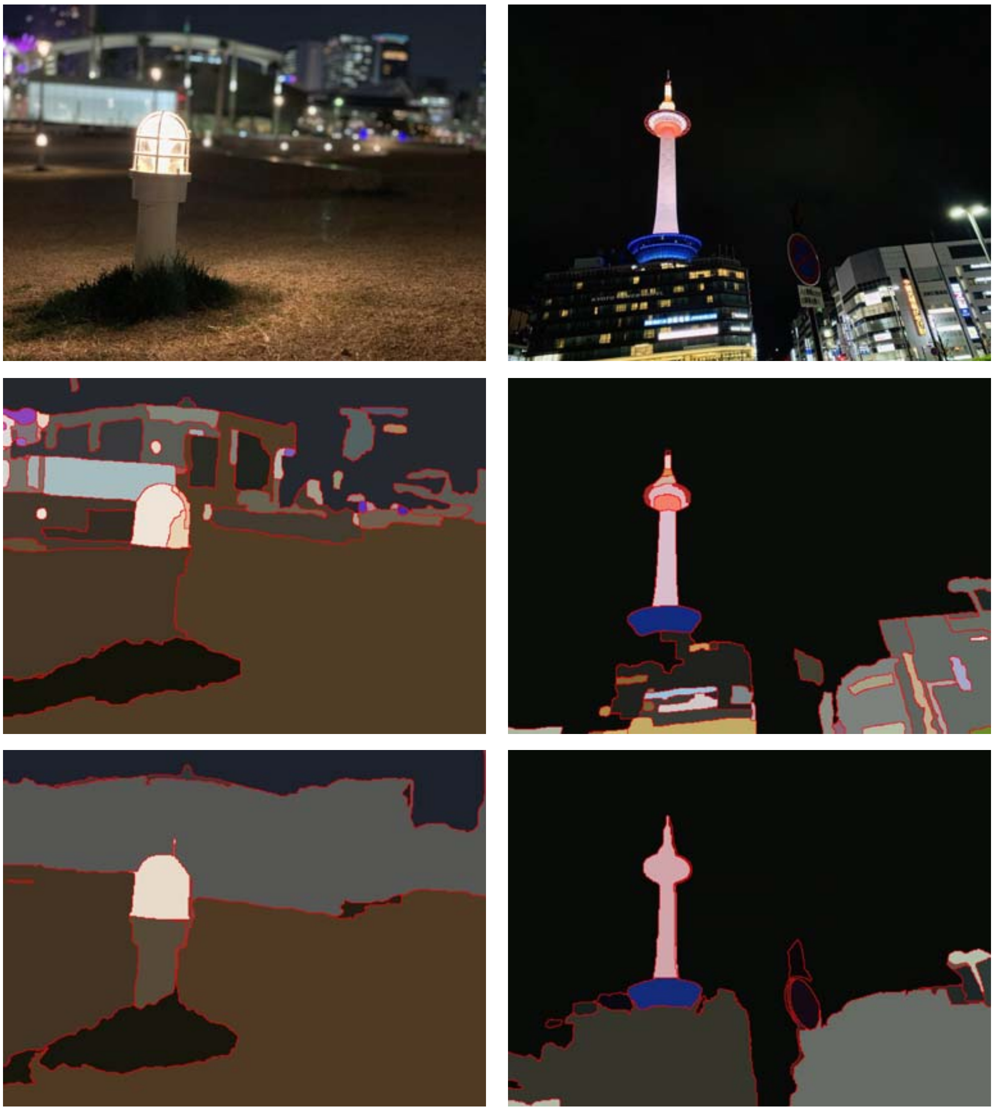

Figure A.8: Real-world animal image segmentation results. (1^{st} row): original images. Results produced by (2^{nd} row): gPb-OWT-UCM [4]; (4^{th} row): *DMMSS-FCN(ours)*.

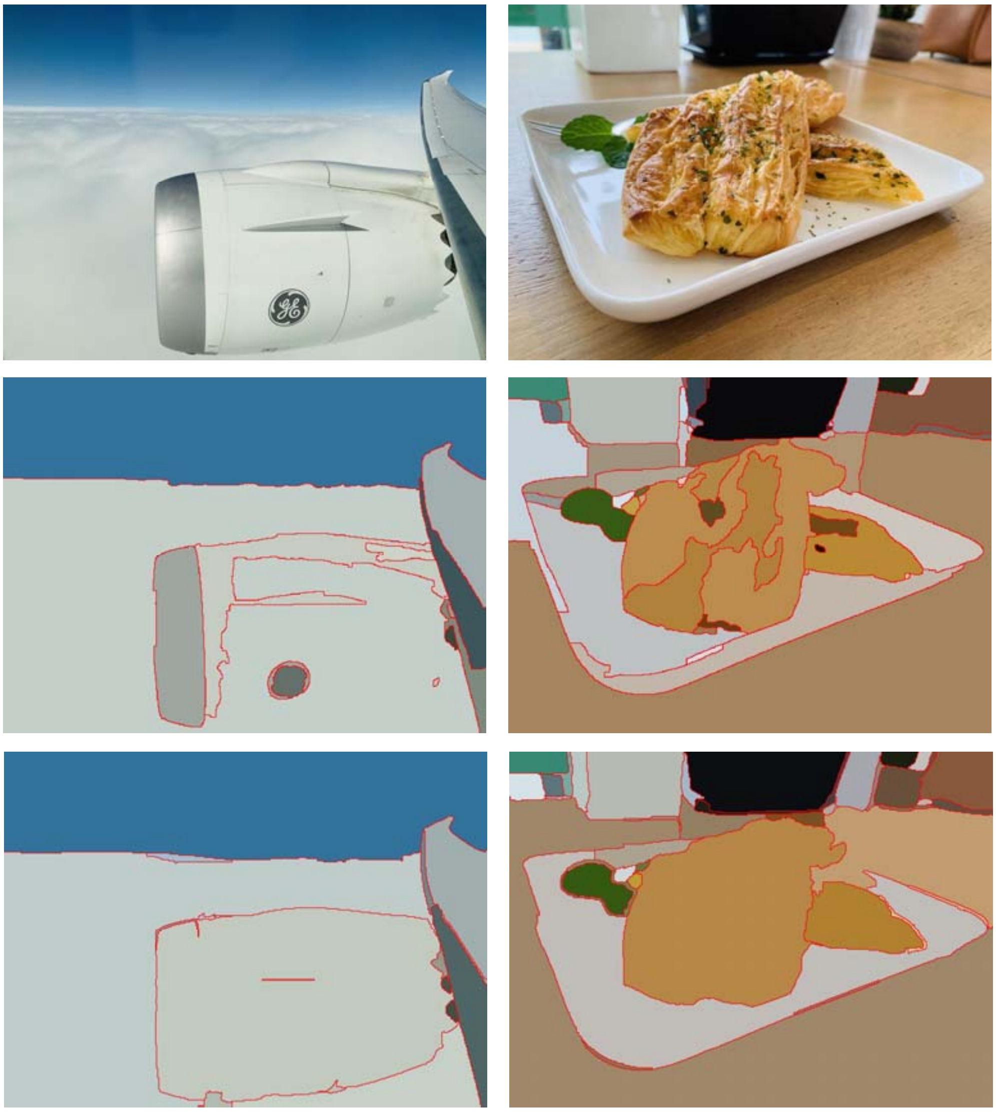

Figure A.9: Real-world animal image segmentation results. (1^{st} row): original images. Results produced by (2^{nd} row): gPb-OWT-UCM [4]; (4^{th} row): *DMMSS-FCN(ours)*.

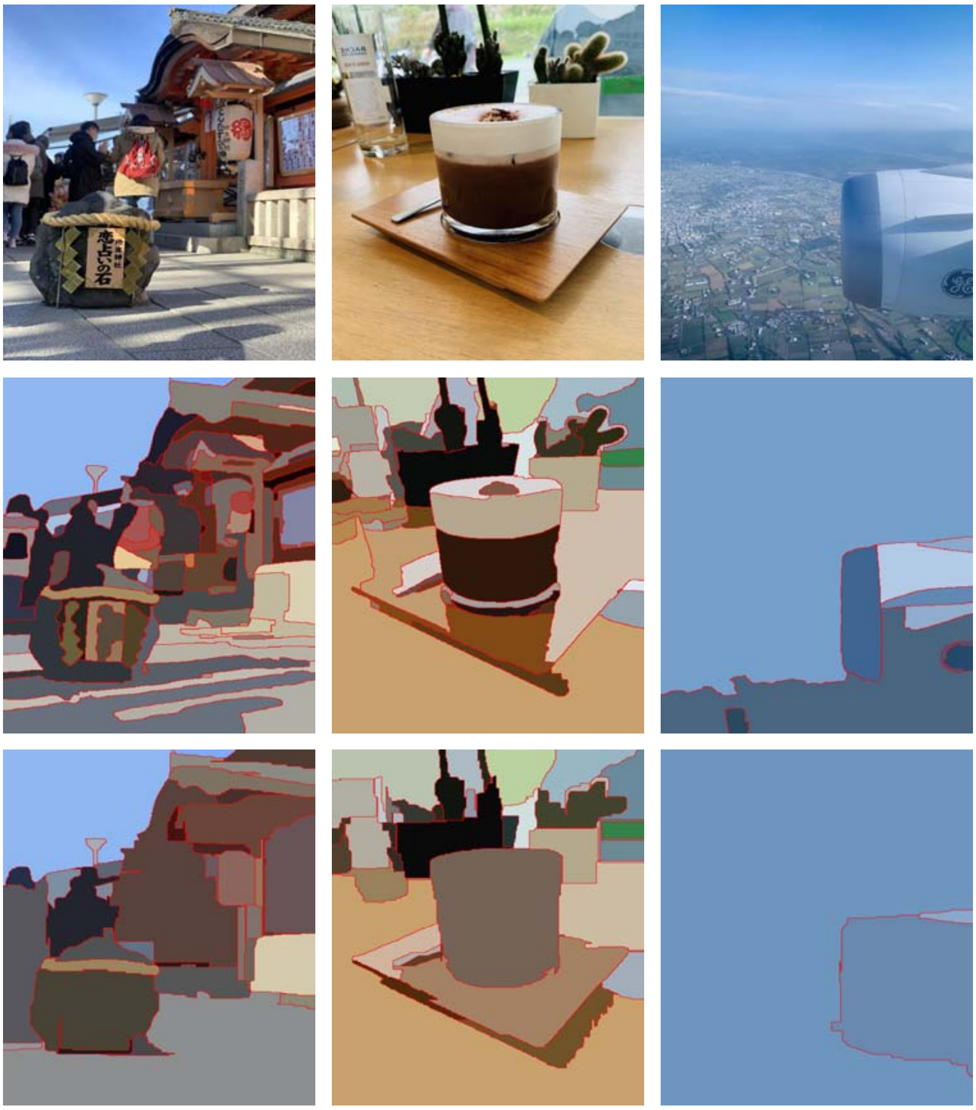

Figure A.10: Real-world animal image segmentation results. (1^{st} row): original images. Results produced by (2^{nd} row): gPb-OWT-UCM [4]; (4^{th} row): *DMMSS-FCN(ours)*.